Resonance Surface Plasmon Spectroscopy: Low Molecular Weight Substrate Binding to Cytochrome P450

Jing Zhao,[†] Aditi Das,[‡] Xiaoyu Zhang,[†] George C. Schatz,*,[†] Stephen G. Sligar,*,[‡] and Richard P. Van Duyne*,[†]

Department of Chemistry, Northwestern University, 2145 Sheridan Road, Evanston, Illinois 60208-3113, and Department of Biochemistry and Chemistry, Beckman Institute for Advanced Science and Technology, University of Illinois Urbana-Champaign, Urbana, Illinois 61801

Received June 1, 2006; E-mail: s-sligar@uiuc.edu; schatz@chem.northwestern.edu; vanduyne@chem.northwestern.edu

Localized surface plasmon resonance (LSPR) nanosensors have been demonstrated as sensitive platforms for the detection of streptavidin,[1] anti-biotin,[2] concanavalin,[3] Alzheimer disease bio-markers,[4] and many other biorecognition events.[5] Sensing is accomplished by monitoring the wavelength shift in the LSPR extinction or scattering maximum (λ_{max}) induced by the binding of target analytes to the nanoparticle surface. The concentration of target analytes is quantitatively related to the shift in λ_{max}. In these cases, however, the analytes were optically transparent; and consequently, the observed shift was only weakly dependent on the LSPR λ_{max}.[1−4] Since many biomolecules contain visible chromophores, it is important to broaden the scope of LSPR sensing by exploring electronically resonant adsorbates in biosensing events. When resonant molecules are adsorbed on nanoparticles, the induced LSPR shift is found to be strongly dependent on the spectral overlap between the electronic resonance of the adsorbates and the plasmon resonance of the nanoparticles.[6] Specifically, a large red-shift occurs when the nanoparticles' LSPR is located at a slightly longer wavelength than the adsorbate's molecular resonance wavelength, that is, a factor of 3 greater than when the LSPR is distant from the molecular resonance. This resonant LSPR response opens up the possibility of detecting the binding of a low molecular weight analyte to a protein receptor adsorbed on a nanoparticle. Herein, we present a proof-of-concept experiment for the binding of camphor ($C_{10}H_{16}O$, molecular weight (M_r) = 152.24 g·mol^{-1}) to cytochrome P450cam protein (CYP101). This system was selected because the electronic structure changes that occur when substrate binds have been well characterized.[7,8]

Cytochrome P450s are essential for steroid hormone biosynthesis and are involved in the metabolism of xenobiotics. Many drug molecules, for example, metyrapone, fluconazole, and cimetidine,[9] inhibit cytochrome P450, thereby leading to a decrease in metabolism which can cause adverse toxicity. The development of an ultrasensitive, label-free detection method for binding of the molecules to cytochrome P450s would, therefore, have a significant impact on drug discovery research.[10−12] CYP101 is a specific member of this P450 superfamily catalyzing the stereospecific hydroxylation of camphor as the first step in the utilization of this terpene as a sole source of carbon and energy in the soil organism *Pseudomonas putida*. Figure 1A shows the UV−vis absorption spectra of camphor-free (green solid line) and camphor-bound (pink dashed line) oxidized CYP101 in phosphate buffer (pH = 7.4). When camphor binds to CYP101 with the heme iron in its +3 oxidation state, CYP101(Fe^{3+}), the Soret absorption band peak of CYP101 blue-shifts by 26 nm from its low spin state at 417 nm (extinction coefficient ϵ = 115 mM^{-1} cm^{-1}) to its high spin state
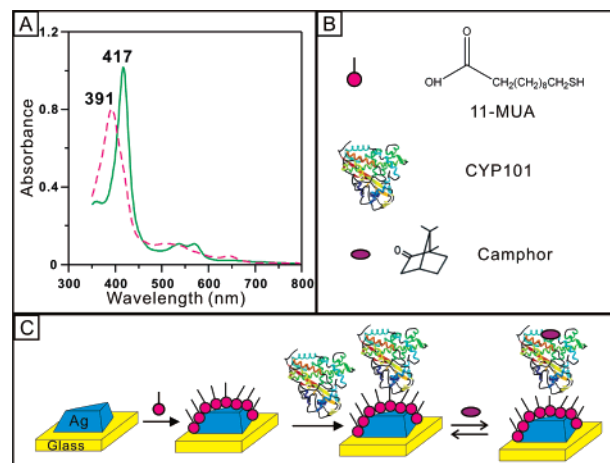

Figure 1. (A) UV−vis absorption spectra of CYP101(Fe^{3+}) (green solid line) with a Soret band at 417 nm (low spin) and camphor-bound CYP101-(Fe^{3+}) (pink dashed line) with a Soret band at 391 nm (high spin); (B) schematic notations of 11-MUA, CYP101, and camphor; (C) schematic representation of CYP101 protein immobilized Ag nanobiosensor, followed by binding of camphor. The Ag nanoparticles are fabricated using NSL (nanosphere lithography) on a glass substrate.

at 391 nm (ϵ = 102 mM^{-1} cm^{-1}). The cause of this peak shift is the displacement of water coordinated with the Fe^{3+} in CYP101 by camphor which shifts the spin state of the heme iron from low to high spin.[7,8,13]

Nanosphere lithography (NSL) fabricated Ag nanoparticles were used as the LSPR sensing platform.[1,2,4,14] To immobilize Fe^{3+}-CYP101 onto Ag nanoparticles, a self-assembled monolayer (SAM) of 11-mercaptoundecanoic acid (11-MUA) (Figure 1B) was used to modify the nanoparticles. With the aid of 1-ethyl-3-[3-dimethy-aminopropyl] carbodiimide hydrochloride, the amine groups on the CYP101(Fe^{3+}) were covalently bound to the carboxyl groups on 11-MUA.[1] Then, the samples were exposed to a 200 μM camphor solution. Since the dissociation constant K_d is 0.61 μM, this concentration saturates all binding sites in Fe^{3+}CYP101.[7,13,15] The experimental procedure is summarized in Figure 1C.

Each step of the functionalization of the samples was monitored using UV−vis extinction spectroscopy in a N_2 environment. Parts A and B of Figure 2 show two sets of representative LSPR spectra. In Figure 2A, after incubation in 11-MUA, the LSPR extinction wavelength, $\lambda_{max,SAM}$ was measured to be 636.1 nm. The sample was then incubated in CYP101(Fe^{3+}) solution. The LSPR of CYP101(Fe^{3+}) modified nanoparticles, $\lambda_{max,CYP101}$, red-shifted by 13.2 nm to 649.3 nm. Next, the sample was exposed to a camphor solution, and the LSPR, $\lambda_{max,CYP101−Cam}$, blue-shifted by 8.7 nm to 640.6 nm. A parallel experiment was conducted using the nano-particles with $\lambda_{max,SAM}$ close to but slightly greater than the
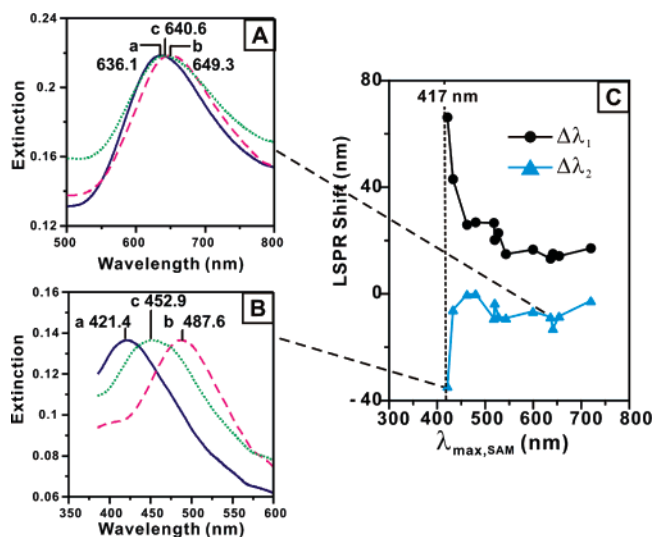
Figure 2. UV-vis extinction spectra of each step in the surface modification of NSL fabricated Ag nanoparticles and the wavelength-dependent LSPR shift plots. All extinction measurements were collected in a N_2 environment. A 200 μM camphor buffer solution was used: (A) a series of UV–vis extinction spectra of Ag nanoparticles (a) $\lambda_{max,SAM}$ = 636.1 nm, (b) $\lambda_{max,CYP101}$ = 649.3 nm, and (c) $\lambda_{max,CYP101-Cam}$ = 640.1 nm; (B) a series of UV–vis extinction spectra of Ag nanoparticles (a) $\lambda_{max,SAM}$ = 421.4 nm, (b) $\lambda_{max,CYP101}$ = 487.6 nm, and (c) $\lambda_{max,CYP101-Cam}$ = 452.9 nm; (C) plots of LSPR shifts versus $\lambda_{max,SAM}$ where $\Delta\lambda_1 = \lambda_{max,CYP101} - \lambda_{max,SAM}$ (shift on binding CYP101), and $\Delta\lambda_2 = \lambda_{max,CYP101-Cam} - \lambda_{max,CYP101}$ (shift on binding camphor). The vertical black dotted line denotes the molecular resonance of $Fe^{3+}CYP101$ at 417 nm.

molecular resonance of the CYP101(Fe^{3+}) ($\lambda_{max,SAM}$ = 420 nm; the molecular resonance of CYP101(Fe^{3+}) is at 417 nm). In this case, dramatic wavelength shifts were observed (shown in Figure 2B). Specifically, the LSPR red-shifted by 66.2 nm to 487.6 nm after incubation in CYP101(Fe^{3+}), and then blue-shifted by 34.7 nm to 452.9 nm upon the substrate binding of camphor.

On the basis of the aforementioned results, it is clear that the LSPR shifts vary strongly with $\lambda_{max,SAM}$. To study this, experiments were conducted to measure the LSPR response of nanoparticles while varying the initial LSPR wavelength. The LSPR peaks were controlled by changing the nanosphere diameter and the deposited metal film thickness.[16] In general, an increase in nanosphere diameter and/or a decrease in metal film thickness result in a red-shift in LSPR. Figure 2C shows the wavelength-dependent plots of $\Delta\lambda_1$ (black line with dots), and $\Delta\lambda_2$ (blue line with triangles) versus $\lambda_{max,SAM}$. The values of $\Delta\lambda$ were calculated from the following equations:

$$\Delta\lambda_1 = \lambda_{max,CYP101} - \lambda_{max,SAM} \quad (1)$$

$$\Delta\lambda_2 = \lambda_{max,CYP101-Cam} - \lambda_{max,CYP101} \quad (2)$$

Here, a positive wavelength shift indicates a red-shift and a negative wavelength shift indicates a blue-shift. When the $\lambda_{max,SAM}$ is located at wavelengths longer than the CYP101(Fe^{3+}) resonance (>460 nm), an average shift of ~19 nm is observed for $\Delta\lambda_1$, and ~ −6 nm for $\Delta\lambda_2$. However, when $\lambda_{max,SAM}$ is at a slightly longer wavelength than the CYP101(Fe^{3+}) resonance (the results shown in Figure 2B), amplified shifts are observed for $\Delta\lambda_1$ (amplified magnitude ~340%) and $\Delta\lambda_2$ (~550%).

These results are remarkable owing to both the magnitude of the shifts and the shift direction. In previously reported studies of LSPR response to the binding of nonresonant proteins to the nanoparticles, we always observed a red-shift in LSPR wave-

length.[1,4] Similarly, we observe that the LSPR red-shifts from $\lambda_{max,SAM}$ upon binding of either CYP101(Fe^{3+}), or camphor bound CYP101(Fe^{3+}). However, the exposure of CYP101(Fe^{3+}) modified nanoparticles to camphor results in a blue-shift (i.e., $\Delta\lambda_2$). If camphor were a noninteracting adsorbate added to CYP101(Fe^{3+}), the local refractive index around the nanoparticles would increase, resulting in a red-shift in the LSPR peaks. However, blue-shifts are found for a variety of nanoparticles with different $\lambda_{max,SAM}$ (Figure 2C). This shows that substrate binding to CYP101(Fe^{3+}) involves a change in the electronic state of the protein, and since this state is at a shorter wavelength than in CYP101(Fe^{3+}), the $\lambda_{max,CYP101-Cam}$ is blue-shifted relative to $\lambda_{max,CYP101}$.

The tunability of the localized surface plasmon resonance has been successfully exploited as a signal transduction mechanism for the detection of substrate binding. Indeed, this is the first demonstration that the binding of a small molecule (camphor) to a protein (CYP101(Fe^{3+})) can generate a LSPR spectral change. Amplified spectral response to substrate binding is achieved when the LSPR of the silver nanosensor is optimized to be close to the molecular resonance of the protein. This study demonstrates that strong coupling between the molecular resonance and the intrinsic LSPR of the nanoparticles results in an amplified LSPR shift that is modulated by substrate binding, providing further insight into possible uses of plasmon resonance spectroscopy. Application of this finding to the screening for inhibitors of human cytochrome P450s is under investigation on the basis of these results. It is foreseeable that this discovery will provide guidance to the design and optimization of refractive index based sensing for biological targets with resonant chromophores.

Supporting Information Available: Detailed description of the experimental methods is available. This material is available free of charge via the Internet at http://pubs.acs.org.

References

(1) Haes, A. J.; Van Duyne, R. P. *J. Am. Chem. Soc.* **2002**, *124*, 10596–10604.
(2) Riboh, J. C.; Haes, A. J.; McFarland, A. D.; Yonzon, C. R.; Van Duyne, R. P. *J. Phys. Chem. B* **2003**, *107*, 1772–1780.
(3) Yonzon, C. R.; Jeoungf, E.; Zou, S. L.; Schatz, G. C.; Mrksich, M.; Van Duyne, R. P. *J. Am. Chem. Soc.* **2004**, *126*, 12669–12676.
(4) Haes, A. J.; Chang, L.; Klein, W. L.; Van Duyne, R. P. *J. Am. Chem. Soc.* **2005**, *127*, 2264–2271.
(5) Dahlin, A.; Zach, M.; Rindzevicius, T.; Kall, M.; Sutherland, D. S.; Hook, F. *J. Am. Chem. Soc.* **2005**, *127*, 5043–5048.
(6) Haes, A. J.; Zou, S. L.; Zhao, J.; Schatz, G. C.; Van Duyne, R. P. *J. Am. Chem. Soc.*, published online Aug 2, 2006, http://dx.doi.org/10.1021/ja063575q.
(7) Lipscomb, J. D.; Gunsalus, I. C. *Drug Metab. Dispos.* **1973**, *1*, 1–5.
(8) Schlichting, I.; Berendzen, J.; Chu, K.; Stock, A. M.; Maves, S. A.; Benson, D. E.; Sweet, B. M.; Ringe, D.; Petsko, G. A.; Sligar, S. G. *Science* **2000**, *287*, 1615–1622.
(9) *Cytochrome P450: Structure, Function, and Mechanism,* 3rd ed.; Kluwer Academic/Plenum: New York, 2005; p 247–322.
(10) Guengerich, F. P. *J. Biol. Chem.* **1991**, *266*, 10019–10022.
(11) Guengerich, F. P. *Annu. Rev. Pharmacol. Toxicol.* **1999**, *39*, 1–17.
(12) Spatzenegger, M.; Jaeger, W. *Drug Metab. Rev.* **1995**, *27*, 397–417.
(13) Sligar, S. G. *Biochemistry* **1976**, *15*, 5399–5406.
(14) Malinsky, M. D.; Kelly, K. L.; Schatz, G. C.; Van Duyne, R. P. *J. Am. Chem. Soc.* **2001**, *123*, 1471–1482.
(15) Denisov, I. G.; Makris, T. M.; Sligar, S. G.; Schlichting, I. *Chem. Rev.* **2005**, *105*, 2253–2277.
(16) Haynes, C. L.; Van Duyne, R. P. *J. Phys. Chem. B* **2001**, *105*, 5599–5611.

JA0636082